PETROPHYSICS, VOL. 43, NO. 3 (MAY-JUNE 2002); P. 153–171; 33 FIGURES

Practical Application of Geostatistical Scaling Laws for Data Integration

P. Frykman[1] and C.V. Deutsch[2]

ABSTRACT

Reconciling data from different scales is a long-standing problem in reservoir characterization. Data from core plugs, well logs of different types, and seismic data must all be accounted for in the construction of a geostatistical reservoir model. It is inappropriate to ignore the scale difference when constructing a geostatistical model.

Geostatistical scaling laws were devised in the 1960s and 1970s primarily in the mining industry where the concern was mineral grades in selective mining unit blocks of different sizes. These principles can be extended to address problems of core, log and seismic data. The adoption of these classic volume-variance or scaling relationships presents some challenges. Three specific concerns are the ill-defined volume of measurement, uncertainty in the small-scale variogram structure, and non-linear averaging of many responses including acoustic properties and permeability.

We demonstrate the application of volume-variance relations for upscaling and downscaling techniques to integrate data of different scales. Practical concerns are addressed with data from a chalk carbonate reservoir and a clastic reservoir in the Danish North Sea.

INTRODUCTION

The use of what is called the "shared earth model" in reservoir modeling increases the demand for quantitative description and higher resolution in the geological model, and thereby highlights the scaling issues, although most papers ignore the question (Fontaine et al., 1998). The available data almost always measure a different volume scale than the volume of the grid cells used in the numerical model; a strategy to reconcile these differences must be developed. In heterogeneous sequences, knowledge of small scale geological features and the geometry of the low- or high-permeability layers is critical for the flow behavior and upscaling.

Data at scales larger than the traditional core and log scale, e.g. seismic impedances or inverted production data, make it possible to analyze the relation between the spatial correlation at different scales. Impedance data may be used for downscaling to guide the modeling of fine-scale heterogeneity and porosity layering. We must be able to quantitatively analyze the volume-variance aspect of this downscaling. The fine scale structure of the permeability anisotropy is critical in most reservoir applications.

Within the petroleum industry and many other fields where geostatistical models are constructed, the treatment of data at different scales has often been ignored (Almeida and Frykman, 1994) and the problems of the "missing scale" have been discussed or addressed only simplistically (Massonat et al., 1999; Tran, 1995). As a simple approach, core and log data may be averaged in the vertical direction to the scale of the modeling cells (Cox et al., 1995; Frykman and Deutsch, 1996); however, this only partially addresses the scale difference since such simple averaging depends on having representative samples, which is rarely the case and does not account for horizontal averaging. In other examples, a fine-scale model is constructed and then numerically averaged to a larger scale (Damsleth and Tjølsen, 1994; Sweet et al., 1996; Wen and Gomez-Hernandez, 1998). This

Manuscript received by the Editor February 25, 2001
[1]Geological Survey of Denmark and Greenland (GEUS), Copenhagen K, Denmark.
[2]School of Mining and Petroleum Engineering, Department of Civil & Environmental Engineering, University of Alberta, Edmonton, Alberta, Canada

may be applied in a nested fashion due to computational limitations. Attempts have been made to directly incorporate the relations between data of different scales into simulation methods. As an example, the direct simulation of gridblock values conditioned to fine-scale data carried out by cosimulation using cross-covariance between fine- and coarse-scale values has been described (Gomez-Hernandez and Journel, 1994).

An illustration of the different scales shows that the change of scale from core to log measurement volumes is nearly as large as the jump from log volume to that of a geological modeling cell (Figure 1).

The requirement for a scale-dependent and representative variogram and histogram has, to some degree, been overlooked in geostatistical simulation studies and many commercial software packages. The success of existing programs in the petroleum industry is partly founded on the fact that considering some kind of heterogeneity is better than no consideration at all. As numerical models are used more extensively, a more correct treatment of the scaling problem is required.

The ultimate goal of this work is to show how data of different scales may be used simultaneously in the construction of high-resolution geostatistical models. When the different types of data are all "hard," in the sense that they do not contain significant errors or uncertainties relative to the property being modeled, it is possible to use block kriging. Certain data types such as seismic records contain uncertainties related to the great volume of measurement and calibration of the measured acoustic properties to the petrophysical properties of interest. In this case, it is necessary to use block cokriging. The systematic analysis and use of the scaling laws will ultimately lead to development of a multiscale co-simulation approach that is able to honor data at different scales.

Our article begins with a review of volume-variance scaling law theory, followed by an illustration of the application of the scaling laws using a synthetic example. Using core- and well-log-scale data from a Danish chalk-carbonate reservoir the application of the scaling laws is further illustrated using real data. The volume of investigation of well log data is estimated using the statistical parameters of the core and log data, together with their analytical volume-variance relationships. Finally, we show that in cases where the existing data are not at the same scale as the modeling cells used in geostatistical simulations the scaling laws can be used to estimate the correct variogram and correct target histogram

BRIEF REVIEW OF THE VOLUME-VARIANCE SCALING LAWS

Notwithstanding the importance of accounting for data at different scales, the use of geostatistical scaling laws has not seen wide application in petroleum geostatistics. This is due mainly to unfamiliarity with the techniques and the

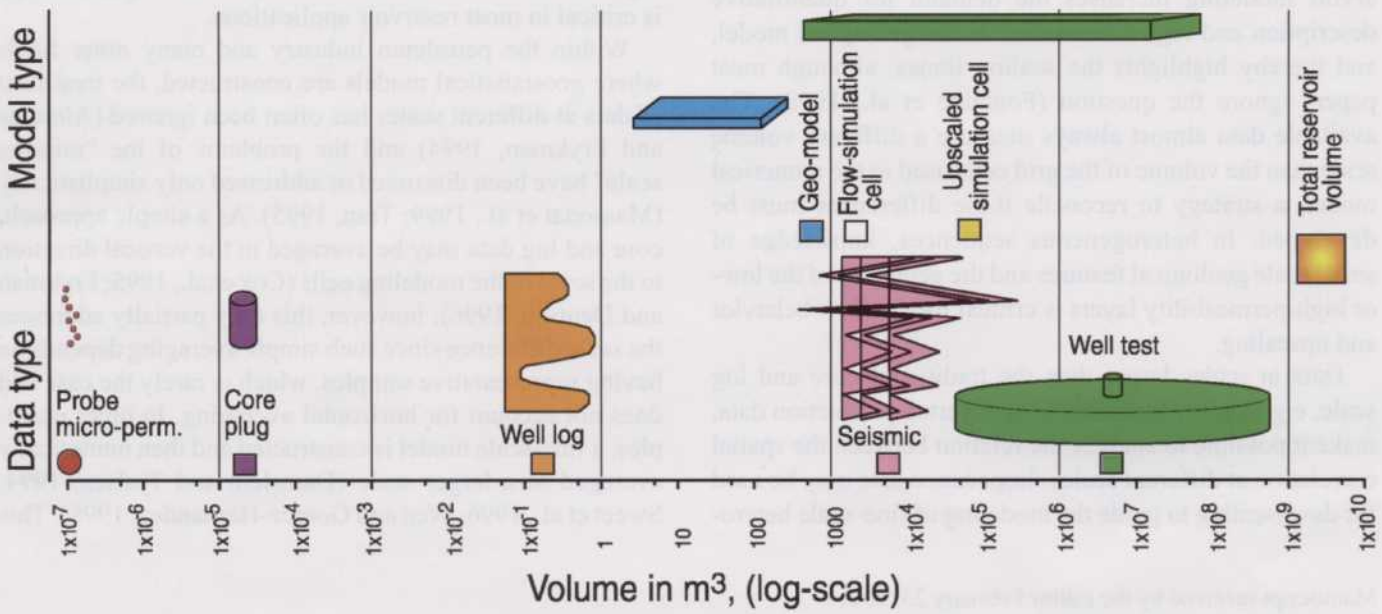

FIG. 1 Illustration of the volume measures (in cubic meters) for the different types of data and model elements. Note that the scale distance between core plug scale and wireline well-log scale is nearly as large as between well-log and reservoir modeling cell volumes.

practical application of the scaling laws. Demonstrating such techniques will address this unfamiliarity.

Our discussion assumes a familiarity with the variogram (Deutsch and Journel, 1998; Goovaerts, 1997; Isaaks and Srivastava, 1989); however, the most important aspects of variogram calculation and modeling are reviewed in the appendix. The scaling laws indicate how statistics such as the histogram and variogram change with the volumetric scale (Frykman and Deutsch, 1999; Kupfersberger et al., 1998). Denoting a smaller volume by $|v|$ and a larger volume by $|V|$, we review some important definitions:

A) The variogram *range a* increases as the size of the sampling volume increases, and a comparison of different scales therefore depends on the difference between the volumes, or $|V| - |v|$. Note that $|V|$ and $|v|$ relate to a size of the volume in a particular direction. For example, if "V" was a block scale of 50 by 50 by 1 m in the X, Y, and Z directions; then, $|V|$ is the size of the block between 70.72 and 1.0 m depending on the direction within the block. The range obviously increases if $|V|$ increases or if $|v|$ decreases. Then, if a_v is the range for the small scale and a_V is the range for the larger scale, we have:

$$a_V = a_v + \left(|V| - |v|\right). \tag{1}$$

B) $\bar{\Gamma}(v,v)$ or the *gamma-bar* value represents the average variogram for vectors where each end of the vector independently describes the volume v. In 3D the gamma-bar values may be expressed by the infamous sextuple integrals of early geostatistics (Journel and Huijbregts 1978, p. 99). The modern approach, however, is to calculate all gamma-bar values numerically.

C) A *nested structure* is in geostatistical jargon a linear combination of basic variogram models and is denoted by C_v^i, $i = 0,\ldots,nst$; where *nst* is the number of individual variogram structures at the scale v.

D) The variance contribution, or *sill*, of each structure C_v^i change by

$$C_V^i = C_v^i \frac{1 - \bar{\Gamma}(V,V)}{1 - \bar{\Gamma}(v,v)}. \tag{2}$$

The variogram used for the calculation of the average variogram values, $\bar{\Gamma}$, is the unit point scale variogram Γ (i.e. variogram with sill of 1.0 and point range a_p), which must be derived from the data at the scale where we have the best knowledge of the correlation structure. The point scale is a theoretical derivation, but can in some cases be substituted by a "quasi point" scale if data exist at a scale much smaller than the investigated volume.

E) The variance of the purely random component of the data, called the *nugget effect*, is inversely related to volume, i.e.,

$$C_V^0 = C_v^0 \frac{|v|}{|V|} \tag{3}$$

where C_V^0 is the nugget effect at the scale V.

As scale increases, the range of correlation increases, and the variogram sill decreases. The variance decreases as the volume increases; high and low values are averaged out as the volume of investigation or measurement increases. As the variance decreases the variogram structure therefore changes as described. The scaling relations are established under the assumptions that: 1) the shape of the variogram (i.e., spherical, Gaussian, etc.) does not change; 2) the averaging is performed with non-overlapping volumes, and 3) the variable scales in a linear fashion (Journel and Huijbregts, 1978). The last assumption has so far prevented the use of the conventional scaling laws on parameters like permeability, although some regularities of permeability scaling have been documented (Tidwell and Wilson, 2000) and permeability may scale linearly after a "power-law" transformation.

These scaling laws have recently been implemented in software that can be used easily for analyzing the scaling relations between different types of data, and which can aid in the correction of input for geostatistic simulations (Oz et al., 2002).

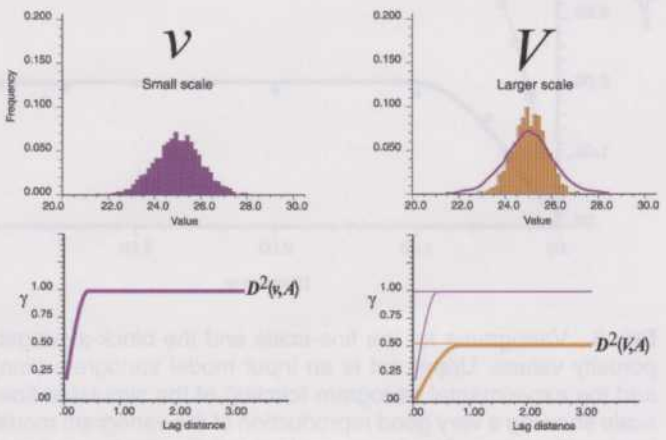

FIG. 2 Schematic illustration of the changes in the histogram, and in the variogram for the variance (sill), and correlation range for data at two different scales.

SCALING RELATIONS WITH SYNTHETIC EXAMPLE

In order to show the application of the scaling rules for data obtained at different scales, a synthetic fine-scale 1-D

model is generated that will be used as a "true" basic model. The program SASIM, based on simulated annealing (Deutsch and Journel, 1998), has been used to simulate the model using a target histogram and a spherical variogram model. The scale of the 1-D modeling cell is 0.02 m in order to mimic the fine-scale geological information normally available from core plugs. The resulting model is illustrated in Figure 3.

Block average values for each non-overlapping 0.5 m segment are calculated from the fine scale data, and will mimic approximately the scale of a well-log. The resulting averaged data are also shown in Figure 3. A similar use of simulated data has been applied to study changes in variability due to the filtering effect of well-logs (Jennings, 1999).

The histograms at the two different scales are shown in Figure 4. The variance is reduced significantly from 3.57 to 1.99 due to the averaging. The variogram model used for simulating the synthetic case is a spherical model with 0.54 m range and zero nugget. The sill value of 3.6 is supplied by the target histogram for the simulation. The simulation is seen to closely reproduce the variogram model (Figure 5).

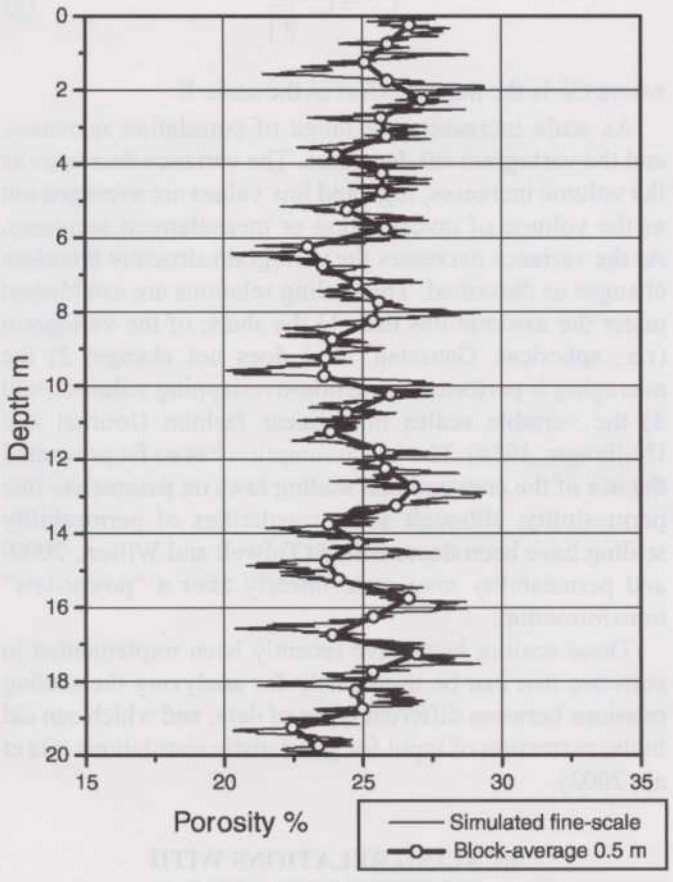

FIG. 3 Profile of the simulated porosity data at 0.02 m scale (thin line), and the block-averaged values for 0.50 m scale (points and thick line).

Application of Scaling Laws for Prediction of Coarse-Scale Variogram from Fine-Scale Variogram

The theoretically derived variogram for coarse-scale may be calculated by the scaling laws and compared to the experimental variogram from the block-averaged coarse-scale data. The closeness of the match is a measure of the efficacy of the scaling relations. We use the fine-scale vari-

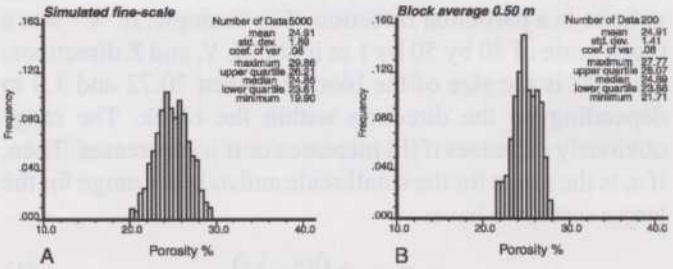

FIG. 4 Histograms of: (A) The simulated fine-scale porosity; (B) The porosity values after block averaging over 0.50 m intervals.

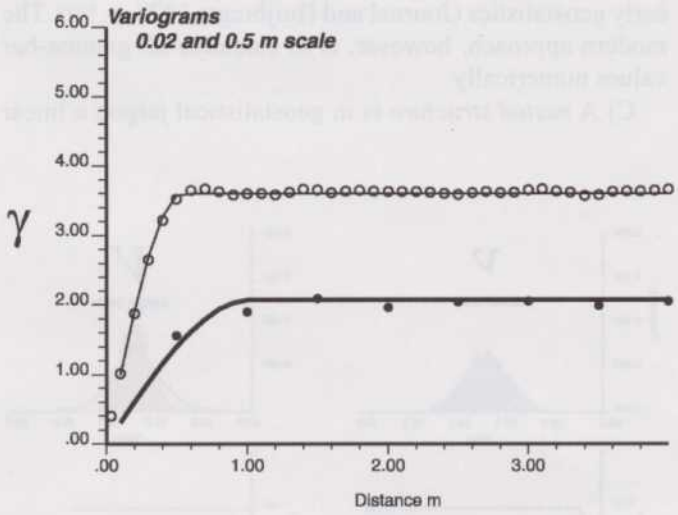

FIG. 5 Variograms for the fine-scale and the block-averaged porosity values. Upper set is an input model variogram (line) and the experimental variogram (circles) of the simulated fine-scale showing a very good reproduction of the variogram model by the simulation. The lower set is the theoretically predicted variogram from applying the scaling laws (line) and the experimental variogram calculated from the block-average porosity values (dots).

ogram model, that is, the spherical variogram structure with 0.54 m range and sill of 3.6.

As stated above in equation (1), the coarse-scale variogram range a_V may be calculated based on the fine-scale range a_v, that is, $a_V = a_v + (|V| - |v|)$. Where v is the fine-scale of dimension 0.02 m and V is the coarse-scale at 0.50 m resolution. This results in a range correction for the variogram from the fine-scale to coarse-scale as follows

$$a_V = 0.54 + (0.50 - 0.02) = 1.02 \text{ m}$$

The sill of each basic structure in the variogram model is modified as in equation (2). The required $\bar{\Gamma}(0.02,0.02)(v)$ and $\bar{\Gamma}(0.5,0.5)(V)$ values can be calculated numerically as

$$\bar{\Gamma}(v,v) = 0.0192 \text{ and } \bar{\Gamma}(V,V) = 0.436.$$

The variance for the fine-scale data for the structure $C_v = 3.6$, and therefore the log-scale sill for the structure is derived with equation (2) as $C_V = 3.6(1 - 0.436/1 - 0.0192) = 2.07$. The comparison of the theoretically predicted coarse-scale variogram and the experimental variogram obtained from the block-averaged data is illustrated in Figure 5, showing a very good agreement.

In order to further illustrate these scaling laws, the procedure has been applied at coarse scale resolutions of 1.0, 2.0 and 4.0 m. The comparison between the theoretical predictions and the experimental variograms is nearly perfect, see Figure 6.

The decrease in sill variance is shown as a function of the averaging volume in Figure 7. However, this function is only valid for this particular model, and heavily depends on the variogram structure at the fine scale level.

Variogram shape change

The synthetic fine-scale model has also been used to investigate how overlapping volume averaging influences the scaling of variograms. For this purpose a moving 0.5 m window filter has been applied with a simple square filter function on the fine scale data. The resulting experimental variogram shows that the variogram structure is changing from the original fine scale spherical model into a more Gaussian-shaped model for the moving average data as seen in Figure 8.

Determination of the averaging volume represented in well-log data

When comparison and scaling of different types of porosity data is attempted, it is necessary to know the averaging volume involved for each type. For porosity estimates derived from well log data, usually from the formation bulk density, the averaging characteristics are not well known (Jennings, 1999). The response function represented in these well-log derived porosity data strongly influences the assumptions made about the averaging volume, and therefore the characteristics are outlined in the following for a

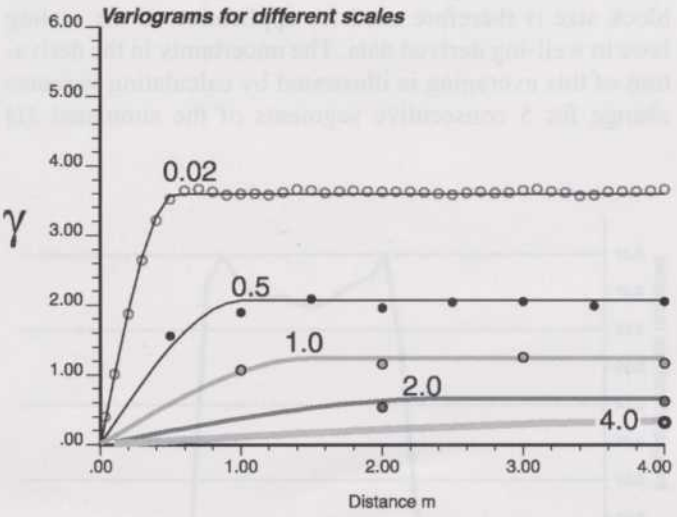

FIG. 6 Comparison of theoretical and experimental variograms for different scales of averaging: 0.02 m is used for cell size for the fine-scale simulation used as starting point for the averaging into 0.5, 1.0, 2.0 and 4.0 m block averages. All predictions show very good match to the experimental variograms shown in dots.

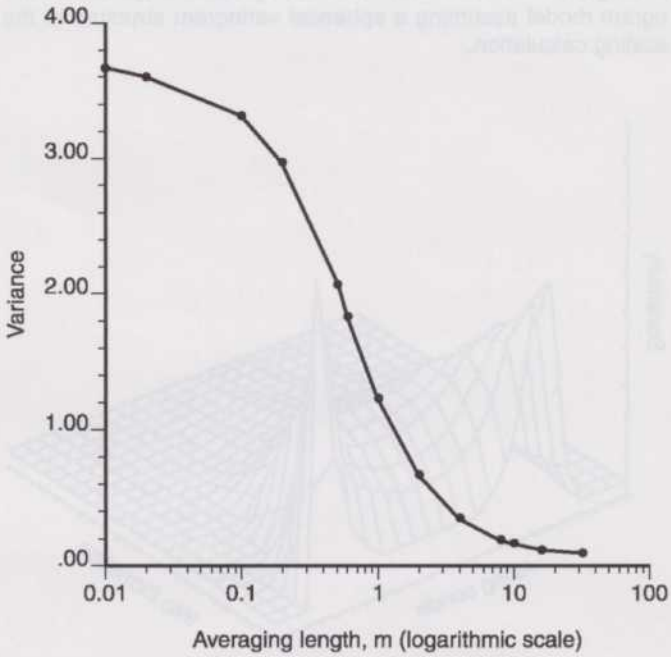

FIG. 7 Illustration of the decrease in variance (sill value) for the theoretically predicted variograms as the length scale of averaging (plotted on log-scale) is varied from 0.01 m to 32.0 m.

commonly supplied logging data type that is the basis for the porosity estimation. The bulk density RHOB data are commonly obtained with an LDT (Litho-Density™ Tool) in North Sea settings and in other areas. The intrinsic response function for this tool is not immediately available, but has been illustrated for similar types of tools (Flaum et al., 1991). The 2D representation of the response function reflects the variable sensitivity according to position and depth into formation of the density measured (Figure 9). This function is then integrated in order to have the 1D response available, given that a layered sequence is investigated (Figure 10).

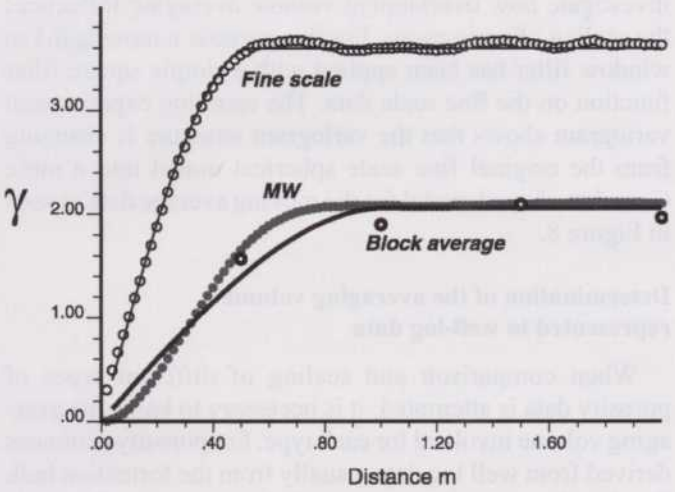

FIG. 8 Model and experimental variograms of the original fine scale simulation (upper line and open dots), and the experimental variogram (MW) for the upscaled data using a moving window average (lower filled dots) indicating a change towards a more Gaussian type variogram model. The lower open dots show the calculated experimental variogram for the block-averaged data. The lower line is the predicted upscaled variogram model assuming a spherical variogram structure in the scaling calculation.

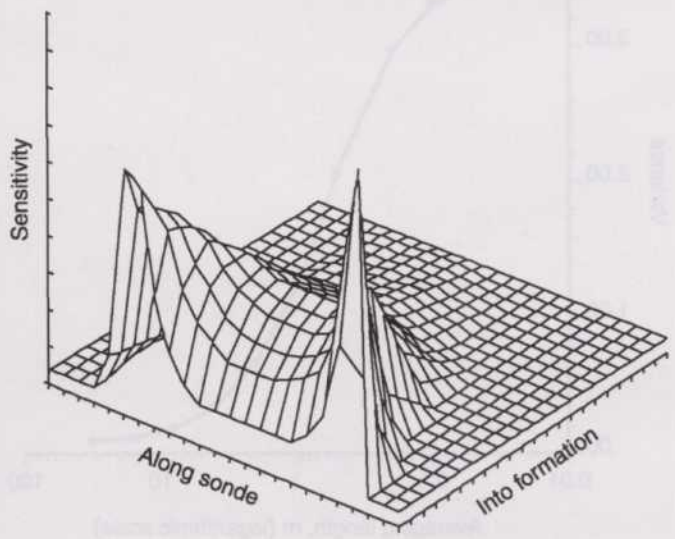

FIG. 9 Illustration of the 2D response function for a hypothetical density detector comparable to what is used in a LDT logging tool (Slightly modified from Flaum et al. (1991)).

A standard processing carried out on the tool count rates is the three-level depth averaging prior to presentation as the RHOB bulk density data that is received as the logging data (Flaum et al., 1989). For standard logging, this processing compares to a square boxcar filter applied on the 6 in. (0.15 m) spaced data. Often this filtering is not reported explicitly, but the boxcar filtering can be recognized in the logging data as a depression in the power-spectrum even when the bulk density has been converted to porosity estimates (Figure 11). The effective response function that corresponds to this 2-step process (tool + filter) of converting fine-scale density (porosity) variations in the formation into the 6 in. (0.15 m) spaced estimates of porosity presented as well-log data therefore can be derived by convolving the intrinsic tool response function with a 3-level (18 in. = 0.45 m) square boxcar filter. The resulting effective response function is shown in Figure 12.

In order to include this information into the scaling laws, it is necessary to derive an "equivalent" non-overlapping block-average block size that approximates the effect of the logging + filtering. This is carried out by applying the effective response function on the simulated fine-scale data and use the resulting variance reduction to estimate an "equivalent" block size (Figure 13). The resulting estimate of 0.62 m block size is therefore used for application of the scaling laws to well-log derived data. The uncertainty in the derivation of this averaging is illustrated by calculating variance change for 5 consecutive segments of the simulated 1D

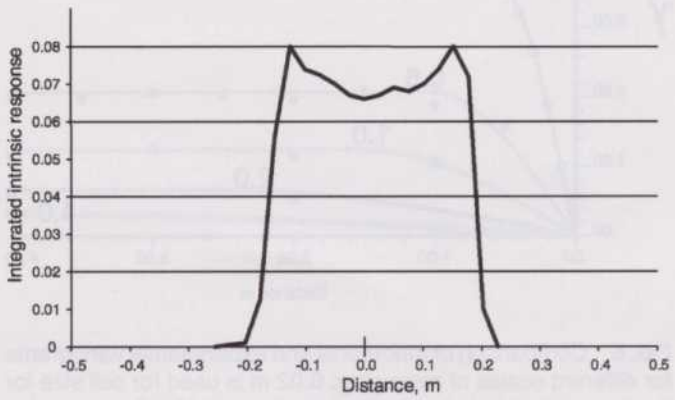

FIG. 10 The intrinsic tool response function for a LDT when bulk density is logged in a layered formation.

model. The spread of these five values shows a corresponding uncertainty in the block size from 0.5 m to 0.8 m averaging length.

SCALING RELATIONS WITH REAL DATA

The scaling laws have been shown to be operational for synthetic data sets created with simple variogram models. The scaling of real data involves several additional aspects that increase complexity. This will be illustrated with two examples.

Chalk reservoir data

Porosity data from an interval in the MFB-7 well from the Dan Field in the Danish North Sea is considered. The Dan Field is an Upper Maastrichtian to Lower Paleogene chalk limestone reservoir, and is characterized by high porosities (30-40%) and generally low permeabilities around 1 mD (Kristensen et al., 1995). Well data from a section covering approximately 18 m of vertical section has been extracted, see Figure 14. Since the well is deviated approximately 32 degrees, any length measures derived from the original wellbore are adjusted by a factor 0.85 (= cos 32°) for true vertical depth. This affects the calculation of the scaling factors and the averaging volume of the logging tool. We chose to work in TVD (True Vertical Depth) space. Our choice is based on the good horizontal continuity in the layered formation drilled; therefore, the variability within the deviated well bore is essentially the same as in the projected vertical section (see Figure 15). The layered aspect also limits the volume scaling relations to essentially a vertically oriented 1D upscaling issue due to the lateral continuity.

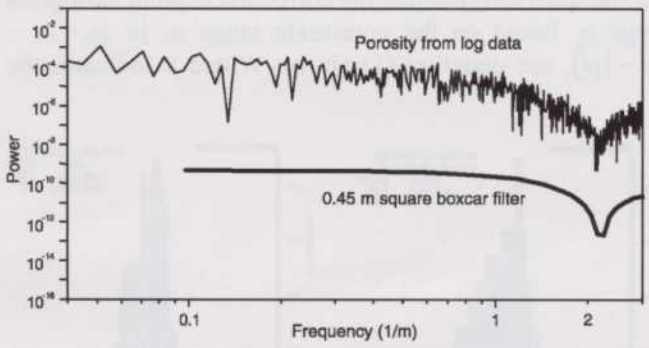

FIG. 11 Power spectrum of the porosity data in the section investigated in the MFB-7 well, and of a 0.45 m square boxcar filter. The comparison indicates that this filtering has been performed on the raw density logging data prior to the derivation of the porosity estimate.

The well data show cyclic porosity variations probably caused by climate variations during deposition of the pelagic chalk material (Scholle et al., 1998; Stage, 2001). The core plug measurements represent a volume of about $5 \times 2 \times 2$ cm (corresponding to a vertical resolution of 0.02 m when the plugs are drilled horizontally). The log measurements represent the averaging length of 0.62 m as developed in the previous section. This corresponds to a 0.53 m vertical section in this particular example. As expected, the core plug porosity values show greater vari-

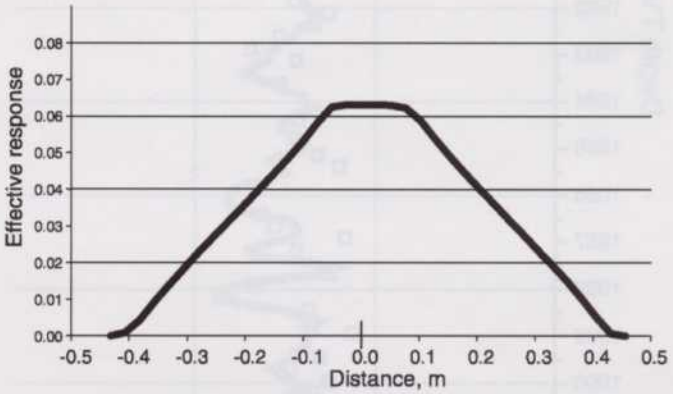

FIG. 12 The effective response function represented in the porosity data derived from logging data. It is the combined effect of the intrinsic log resolution and the succeeding boxcar filtering.

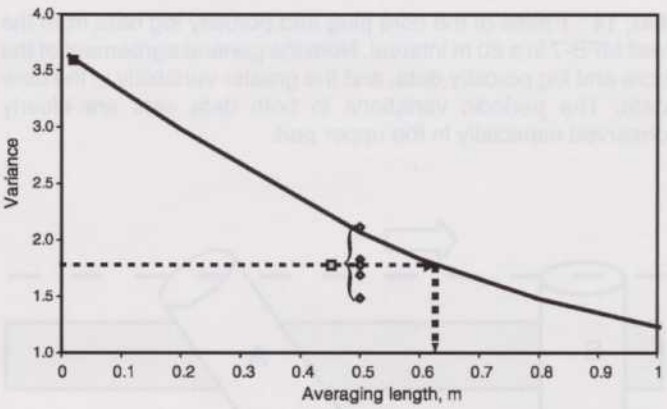

FIG. 13 The curve shows the relation between the variance and averaging length when increasingly larger block averaging lengths are used on fine-scale synthetic data. The points signify the variance for 5 segments of the synthetic data when the effective response function for logging data is applied on the fine-scale data. The average variance intersection of the response function is seen to correspond to a 0.62 m non-overlapping block averaging. The non-overlapping averaging is assumed for application of the scaling laws.

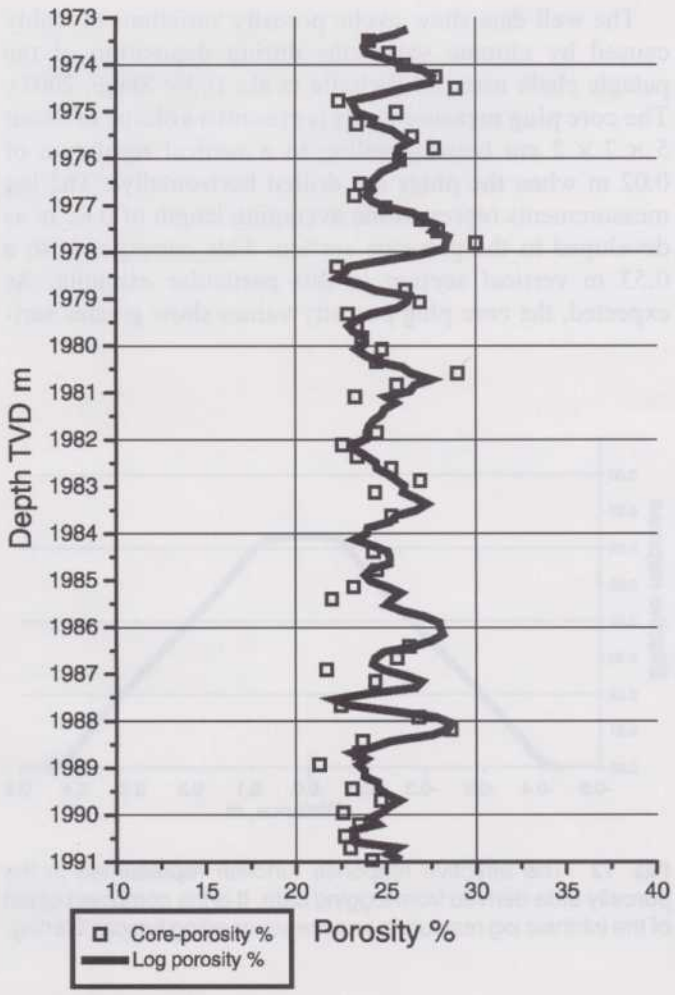

FIG. 14 Profile of the core plug and porosity log data from the well MFB-7 in a 20 m interval. Note the general agreement of the core and log porosity data, and the greater variability in the core data. The periodic variations in both data sets are clearly observed especially in the upper part.

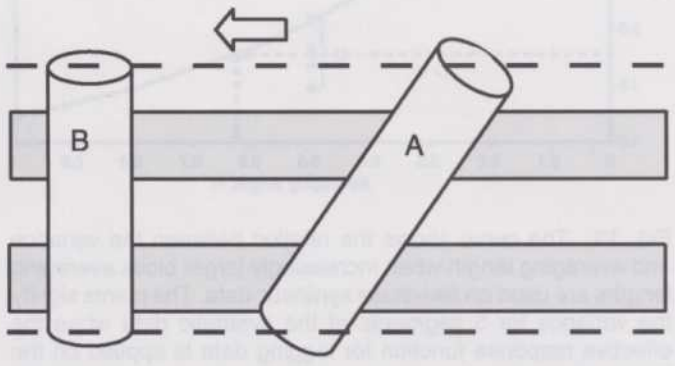

FIG. 15 Schematic illustration of an inclined well and tool volume (length) conversion from measured depth scale (A) to TVD scale (B).

ability than the log porosity values. The histograms shown in Figure 16 illustrate the difference.

Figure 17 shows a cross plot of the core versus log porosity values. The scatter on this plot is attributable to the different measurement volumes, but to a small extent also to the different physics behind the measurements. The cross plot of core and log porosity shows a fair correlation between the two variables, but it is also apparent that the well log data does not represent some of the high porosity layers recorded by the core analysis samples. Whether this is caused by biased sampling for plug material, or an averaging effect of thin beds by the logging method is not known.

The correlation between the core and log porosity also depends heavily on the correct positioning of plug data and the depth adjustment normally carried out to match log and core data. However, when a dubious correlation is seen, an additional evaluation can be performed with the variograms for the two data types. If the variograms are similar and can be connected via the scaling, it probably indicates that the depth match has been poorly performed and should be re-evaluated.

The core-porosity variogram shows clear cyclic variations with a period at about 1.90 m (Figure 18). The variogram model has no nugget effect and two nested structures: (1) a spherical structure with sill equal to 2.82 and range of 0.54 m, and (2) a hole effect model with amplitude 1.2 and peak at 0.95 m. It should be noted that it is somewhat uncertain to model a nested variogram with a hole effect included, due to the interaction between the random function and the periodic signal.

Derivation of Point-Scale Variogram from fine-scale data

The scaling laws developed previously are applied on each nested variogram structure. The core-scale data shows no nugget effect, and therefore no need for scaling of this. For the spherical structure the correction to point variogram range a_p based on the core-scale range a_v is: $a_p = a_v - (|v| - |p|)$, see equation (1) above. Where p indicates the

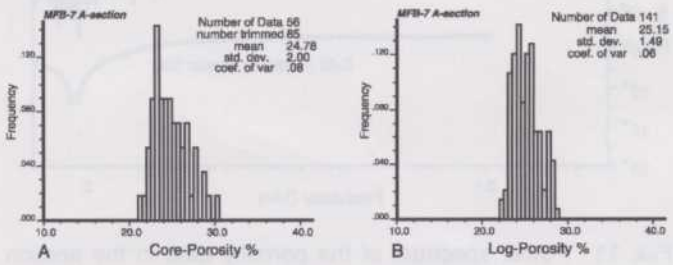

FIG. 16 Histograms of (A) core plug and (B) well log porosity data from the selected interval in the MFB-7 well. Note that the log data has reduced variance compared to the core data.

point scale, which has a length scale of zero and v indicates plug scale, which is 0.02 m. Thus, the corrected range for the spherical nested structure is = 0.54 – (0.02 – 0) = 0.52 m.

For the hole effect structure, the wavelength for the periodic structure is not affected, and the peak distance used for the modeling is kept constant at 0.95 m for the point scale variogram. This is in accordance with the basic principle that filtering a periodic signal cannot affect its wavelength.

The sill of each basic structure is corrected according to equation (2) presented above. The gamma-bar values are calculated numerically for all needed $\bar{\Gamma}(v,v)$ values. For all calculations of mean variogram values we assume one-dimensional averaging of the data. This entails that the well data are only averaged in the vertical direction, which is a fair assumption given that it is a layered formation with large horizontal continuity; therefore, the investigation depth is not to be considered in this case.

The value for $\bar{\Gamma}(v,v)$ for the spherical structure can be calculated using the point-scale variogram description. For calculation of $\bar{\Gamma}(v,v)$, the volume v is defined as the core-plug volume of 5 × 2 × 2 cm with a vertical length scale measure of 2 cm, giving a $\bar{\Gamma}(v,v)_{sph}$ value of 0.019, and a resulting point-scale sill C_p of 2.87 for the spherical structure. This is compared to the core-scale sill value of the spherical structure C_v of 2.82.

The same procedure is used for the hole effect variogram for the amplitude scaling, giving $\bar{\Gamma}(v,v)_{hole}$ = 0.0004, and therefore a virtually unchanged variance contribution of 1.2 for the point scale variogram.

In summary, the theoretically derived point-scale variogram structure has zero nugget and two nested structures: (1) a spherical structure with range 0.52 m and sill of 2.87, and (2) a hole effect structure with peak at 0.95 and a variance contribution of 1.2. This point-scale variogram is the basis for all the gamma-bar calculations performed in connection with the up- and down-scaling using the scaling laws.

Prediction of Log-Scale Variogram from the Core-Scale Variogram

The predicted variogram for log-scale may be calculated and compared to the experimental variogram from log-scale data. The closeness of the match is a measure of the efficacy of the scaling relations described above and the closeness of the real data to the assumptions underlying the scaling relations. The calculations are carried out as described above in the synthetic example.

The core-scale data shows no nugget effect (Figure 18), therefore, there is no nugget effect at larger scales. The range of the log-scale variogram range a_V is calculated based on the core-scale range a_v. Given that the effective averaging length represented in the log data is 0.53 m, this results in a range correction for the spherical structure from the core-scale to log-scale

$$a_{Vsph} = 0.54 + (0.53 - 0.02) = 1.05 \text{ m}.$$

For calculating the predicted variance (sill) values, the

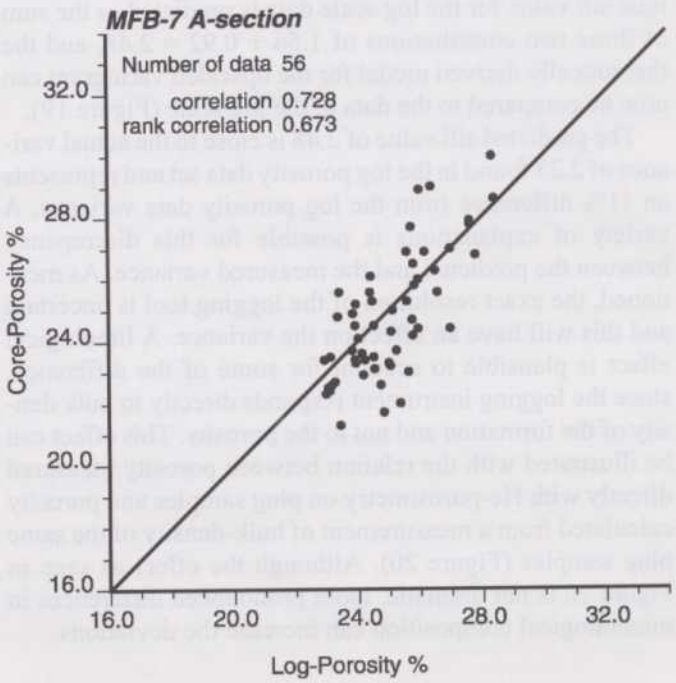

FIG. 17 Cross-plot of log and core porosity data from the MFB-7 interval showing a fair correlation.

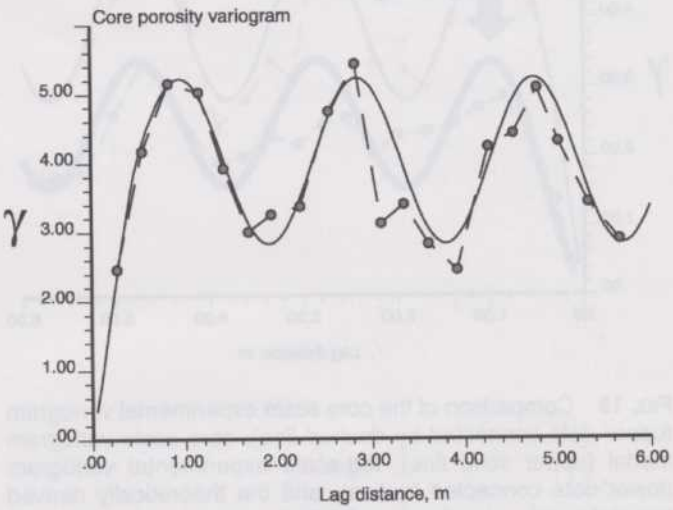

FIG. 18 Experimental variogram of core porosity data from the MFB-7 interval. The experimental variogram has been fitted with a nested model of a spherical and hole effect variogram models.

two structures are treated separately, and the sill of each basic structure in the variogram model is modified as in equation (2).

For the hole-effect structure the peak distance is not changed from the original 0.95 m. The log-scale sill is derived for the spherical structure and equals 1.56. Likewise the sill for the hole effect structure equals 0.92. The total sill value for the log scale data is predicted as the sum of these two contributions of 1.56 + 0.92 = 2.48, and the theoretically derived model for the upscaled variogram can now be compared to the data at the log scale (Figure 19).

The predicted sill value of 2.48 is close to the actual variance of 2.23 found in the log porosity data set and represents an 11% difference from the log porosity data variance. A variety of explanations is possible for this discrepancy between the predicted and the measured variance. As mentioned, the exact resolution of the logging tool is uncertain and this will have an effect on the variance. A lithological effect is plausible to account for some of the difference, since the logging instrument responds directly to bulk density of the formation and not to the porosity. This effect can be illustrated with the relation between porosity measured directly with He-porosimetry on plug samples and porosity calculated from a measurement of bulk-density of the same plug samples (Figure 20). Although the effect as seen in Figure 20 is not dramatic, more pronounced differences in mineralogical composition can increase the deviations.

The difference in variance for the two measures only amounts to 2.5% for these chalk samples, but might reach higher values in more heterogeneous lithologies. This forms at least part of the explanation for the 11% deviation previously shown to occur. It illustrates that the comparison of different data types involves cross-scaling in addition to up- or down-scaling (Corbett et al., 1998). The cross-scaling is the determination of a relationship between two different physical properties, whereas up-scaling is the determination of an effective (or pseudo) property at a scale larger than that of the original measurement. The definition of these terms helps to separate the effects of the geology (largely up-scaling) from that of the physics (largely cross-scaling) in a more systematic manner (Corbett et al., 1998). This is an example of a cross-scaling effect that in some cases might account for a component of the variance difference between the theoretical prediction and the actual data. Finally, the uncertainty in the variogram calculation and modeling have to be considered, although it should be minimized by using a consistent and systematic procedure for variogram modeling (Gringarten and Deutsch, 2001; Frykman, 2001).

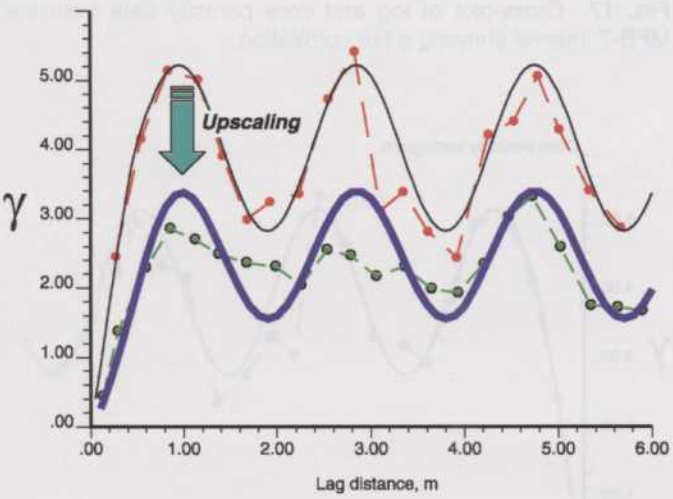

FIG. 19 Comparison of the core scale experimental variogram (upper dots connected by dashed line), core scale variogram model (upper solid line), log-scale experimental variogram (lower dots connected by-line), and the theoretically derived log-scale variogram (lower solid line), using an averaging volume of 0.5 m, which seems to match the actual experimental variogram from the log scale data due to the cross-scaling effect of variance reduction.

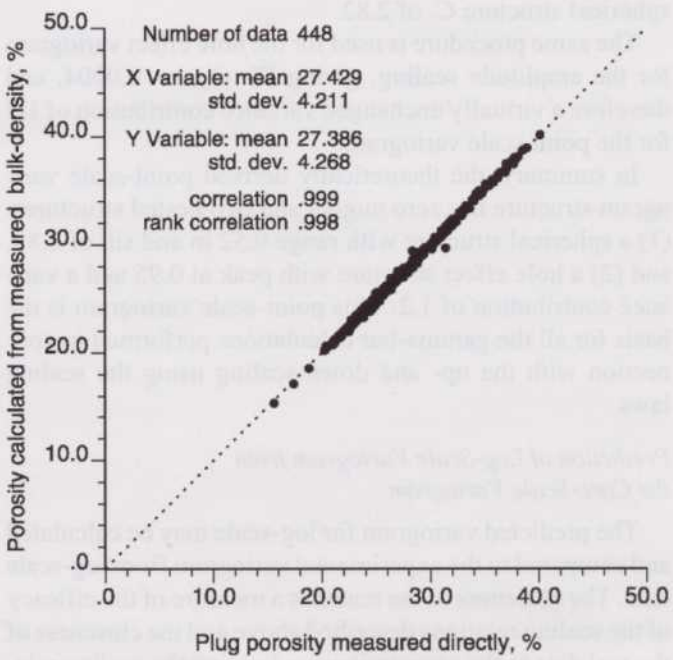

FIG. 20 Illustration of the cross-scaling effect in plug data from a chalk sequence. The plug porosity is measured directly by He-porosimetry, and in addition porosity can be calculated from the directly measured bulk-density assuming a constant grain-density of 2.71. The difference in variance between the two parameters is due to the cross-scaling effect from lithology deviations and measurement errors, effects that are observed even for similar size volumes.

Assessment of Tool Investigation Volume from data at two different scales

Uncertainty is associated with the size and geometry of the volume of averaging in a well-logging instrument; this uncertainty could also occur for other indirect measurement methods such as seismic records. For the current example where the small-scale core data variogram and the experimental log-scale variogram are known, the volume of measurement of the well-log can be estimated. An inverse of the procedure developed above for variance estimation is used. The averaging volume is determined in an iterative fashion until the theoretical gamma-bar prediction of variance matches the actual well-log data derived variance.

Provided a reliable estimate of the point-scale variogram is established, it is possible to calculate the theoretical $\bar{\gamma}(V,V)$ for a range of different volume scales. Then, the actual volume scale can be determined where the theoretical $\bar{\gamma}(V,V)$ matches the experimental $\bar{\gamma}^*(V,V)$.

Background for average variogram value

The point (•) variance within an arbitrary volume v is equal to the mean value $\bar{\gamma}$ of $\gamma(\mathbf{h})$ for all $\mathbf{h}$ and all directions within that volume, where $\gamma(\mathbf{h})$ is the point-scale variogram consisting of all nested structures, that is,

$$\sigma^2(\bullet, v) = \bar{\gamma}(v, v). \tag{4}$$

Furthermore, given a larger region R, the additivity of variance entails that,

$$\sigma^2(\bullet, R) = \sigma^2(\bullet, v) + \sigma^2(v, R) \tag{5}$$

for any volume v. In words, the variance of points • in a region R is equal to the variance of points • within a larger volume v, plus the variance of that larger volume v within the region R.

Consider two different volumes, v and V (e.g., core and log scale volumes). $\sigma^2(\bullet,R)$ is the global stationary point scale variance. Applying relation (5) to volumes v and V, the experimental average variogram $\bar{\gamma}(V,V)$ for the log-scale volume may be expressed as

$$\bar{\gamma}(V,V) = \bar{\gamma}(v,v) + \sigma^2(v,R) - \sigma^2(V,R). \tag{6}$$

In our case

$$\bar{\gamma}(V,V) = \bar{\gamma}(v,v) + 4.02 - 2.23\,.$$

Now $\bar{\gamma}(v,v)$ can be calculated given the real point scale variograms as defined earlier, and as the sum of the contribution from the two structures in the nested model, the $\bar{\gamma}(V,V)$ experimental is obtained as

$$\begin{aligned}\bar{\gamma}(V,V) &= \bar{\gamma}(v,v) + 4.02 - 2.23 \\ &= \bar{\gamma}(v,v)_{sph} + \bar{\gamma}(v,v)_{hole} + 4.02 - 2.23 \\ &= 0.055 + 0.0004 + 4.02 - 2.23 = 1.85\end{aligned}$$

which then gives an independent assessment of the average variogram value within log-scale volumes.

Applying this procedure with the point-scale variogram model derived above leads to the results in Figure 21. The cross plot shows that the experimental value for $\bar{\gamma}^*(V,V)$ of 1.85 matches the theoretical values at a scale of 0.62 m.

This volume-measure of 0.62 m is the length of the vertical averaging, and has to be calculated back to the tool measurement geometry in the inclined wellbore. This gives an effective tool resolution of 0.73 m, which is larger than the 0.62 m that was predicted from the physics of the logging tool. As mentioned there are some additional "uncertainty" that causes the measure derived here to be a "pseudo-source-detector spacing," which accounts for a variety of uncertain effects. A similar estimation of "seismic detection volume" could be derived from knowing the variance of the impedances from well-log data and from the seismic data.

Variogram shape change for real data

The moving average of the density-logging instrument affects the shape of the variograms for the different data types. The experimental variogram for moving average values tends to behave like it has an underlying Gaussian model, even if the original fine-scale data honors a spherical model. In practice this means that in cases where the log data is modeled with a Gaussian variogram model, the

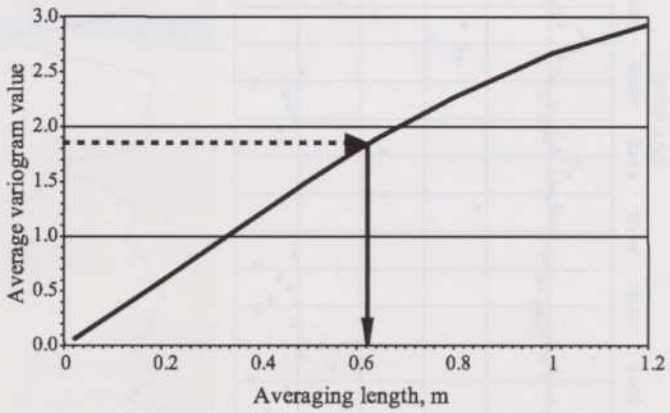

FIG. 21 Cross plot of the theoretical average variogram versus the length scales close to the tool investigation length. The average variogram value of 1.85 is known experimentally permitting an estimate of the scale of investigation, that is 0.62 m, which corresponds to a tool averaging length of 0.72 m in the deviated well.

point-scale variogram most likely could have a less continuous spherical model.

Scaling laws applied to a Middle Jurassic shallow marine sandstone sequence

The Middle Jurassic sandy succession of the Upper Bryne Formation in the Danish Central Graben consists mainly of fluvial to tidally influenced shallow marine sediments. The specific sequence studied here is developed in an estuarine setting in Middle to Late Callovian time (Andsbjerg, 1997). The present data originates from a section in the vertical well West Lulu-2 in the northwestern part of the Danish Central Graben. A section of 17 m has been selected from the Upper Bryne Formation, where mostly shallow marine, tidally influenced, sandy and silty deposits occur. The variability in the porosity reflects the bedded nature of this part of the sequence (Figure 22).

The distribution of the two porosity measures from core plugs and log data is shown in Figure 23. The scatter on the crossplot in Figure 24 is again attributed to the combination of scale difference and the cross-scaling effects.

Downscaling from log to core scale

The exercise is to downscale the log data variogram to the core data. As a start the calculated sill value of the log data is adjusted for the missing variance attributable to the cross-scaling effect. The variance of 8.3 is therefore increased by 11%, which is the amount that was found in the chalk example. This is probably a minimum estimate since small-scale lithological variations are more severe in a clastic sequence than in the fairly clean chalk sequence. The new sill for modeling of the log scale variogram is therefore adjusted to 9.2, and the range for the model variogram is adjusted to fit through the experimental points around the middle part (Figure 25).

After calculating the downscaled variogram we see a good fit to the initial part of the variogram for the core porosity data, and that match to the core data variance is

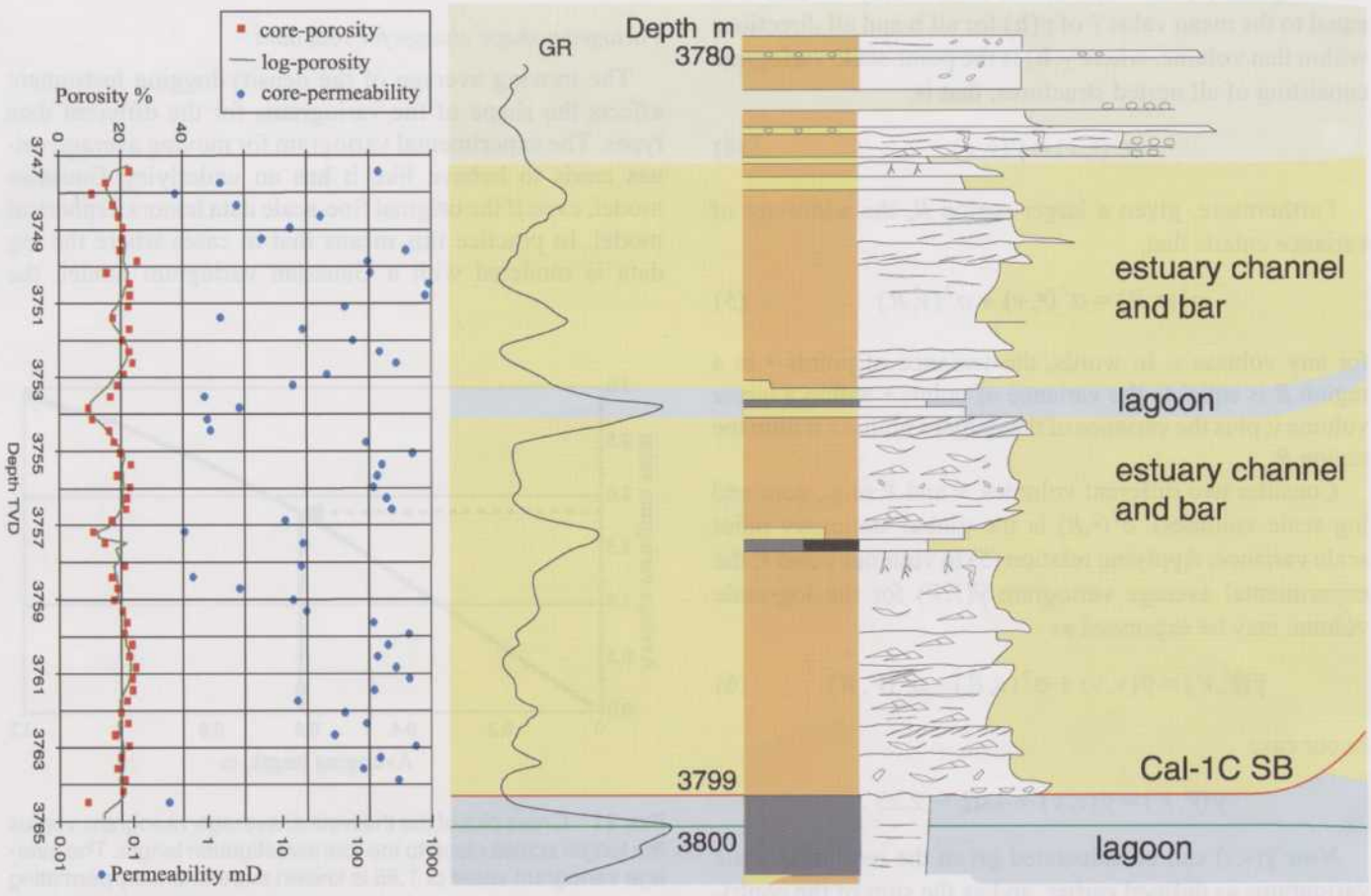

FIG. 22 The analyzed 17 m section in the well West-Lulu-2 showing the succession of facies from an estuarine environment, and the log and core-derived data.

nearly obtained (Figure 26). However, due to the uncertainties in the variogram modeling and the cross-scaling effects, the matching procedure is best performed as an iterative process where the variance and range values are varied until a reasonable compromise is reached.

Although there seems to be a weak hole effect in the experimental variogram, it has not been included in the variogram models. This was decided partly because of the difficulty in obtaining a match to the wavelength of the hole effect if we want to fit the whole variogram. The apparent hole effect is due to a deterministic layering effect in combination with the limited extent of the sequence analyzed.

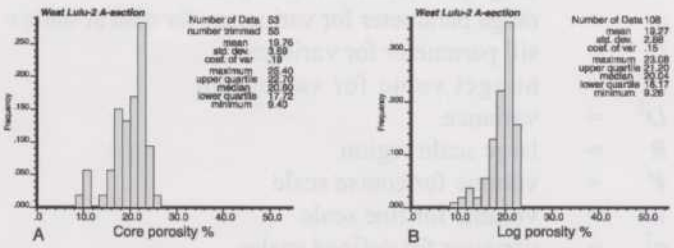

FIG. 23 Histograms of core porosity and log porosity from the interval in the West-Lulu-2 well, showing variance of 13.6 and 8.3 respectively.

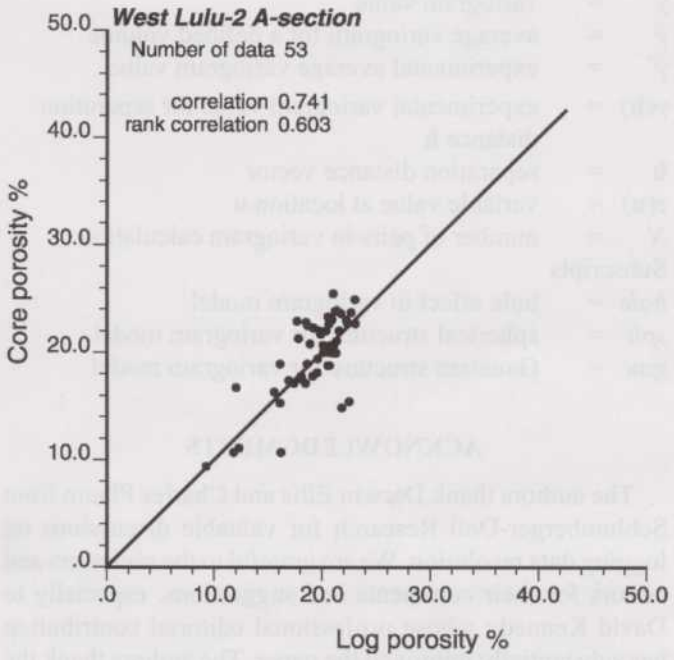

FIG. 24 The scatter on the porosity crossplot is attributed to the combination of scale difference, mismatch of core-log position, and the cross-scaling effects.

DISCUSSION

The case studies illustrate that the comparison of different data types can be achieved via the scaling laws. A good understanding of the averaging volume for the different scales is necessary, and besides the up- and down-scaling, cross-scaling effects must be considered. Cross-scaling is the determination of a relationship between two different physical properties, whereas up-scaling is the determina-

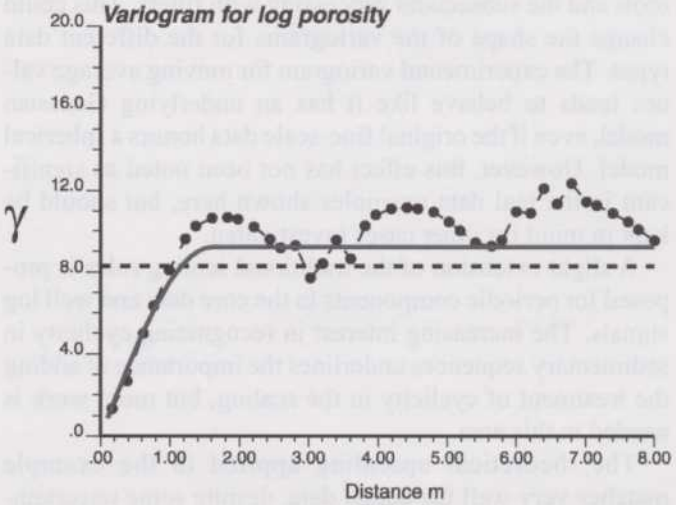

FIG. 25 Experimental variogram for the log porosity (dots). The horizontal line is the stationary variance of 8.3, while the model variogram is fitted with an increased sill value of 9.2 to compensate for the uncertainty and cross-scaling reduction.

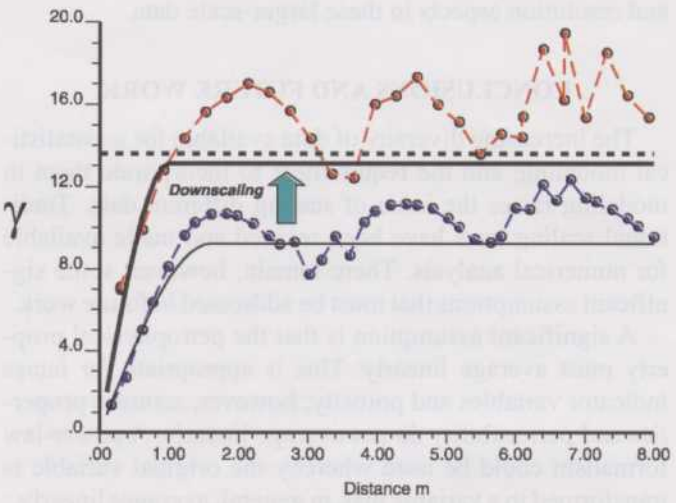

FIG. 26 Experimental variogram for log porosity (lower dots) and core porosity (upper dots) and the model variograms (lines) for downscaling to core plug scale. The horizontal dashed line is the stationary variance of 13.6 for the core plug scale data.

tion of an effective (or pseudo-) property at a scale larger than that of the original measurement. The definition of these terms is a help to separate the effects of geology (largely up-scaling) from that of the physics (largely cross-scaling) in a more systematic manner (Corbett et al., 1998). A better understanding of the magnitude of cross-scaling effects requires the study of more examples of different sedimentary sequences.

An additional effect that causes some uncertainty is the moving average effect during the use of wire-line logging tools and the subsequent processing with filters. This could change the shape of the variograms for the different data types. The experimental variogram for moving average values tends to behave like it has an underlying Gaussian model, even if the original fine-scale data honors a spherical model. However, this effect has not been noted as significant in the real data examples shown here, but should be kept in mind for other cases investigated.

A slight extension of the traditional scaling rules is proposed for periodic components in the core data and well log signals. The increasing interest in recognizing cyclicity in sedimentary sequences underlines the importance of adding the treatment of cyclicity in the scaling, but more work is needed in this area.

The theoretical upscaling applied in the example matches very well the actual data, despite some uncertainties regarding the effects of the cross-scaling variance reduction, and modeling uncertainties. The back-calculation of the averaging volume from the spatial statistics is a useful supplement to analytical calculations and studies regarding logging instrument responses, and could possibly also be applied to seismic data to analyze volumes and resolution aspects in these larger-scale data.

CONCLUSIONS AND FUTURE WORK

The increasing diversity of data available for geostatistical modeling, and the requirement to incorporate them in modeling raises the issue of scaling different data. Traditional scaling laws have been revived and made available for numerical analysis. There remain, however, some significant assumptions that must be addressed in future work.

A significant assumption is that the petrophysical property must average linearly. This is appropriate for facies indicator variables and porosity; however, acoustic properties and permeability do not average linearly. A power-law formalism could be used whereby the original variable is transformed to a variable that, in general, averages linearly.

Another significant assumption in the use of conventional volume-variance relations is that the spatial variability is completely characterized by a stationary random function using 2-point variogram/covariance measures of correlation. No higher order non-linear spatial connectivity is accounted for.

This paper shows that there is a future for scaling laws as an applied tool in the integration of data in reservoir modeling. By simultaneous use of data from the different scales, we achieve more reliable reservoir characterization, and thereby more reliable predictions of reservoir performance.

The scaling laws also have the immediate potential to be incorporated directly into simulation routines, thereby enabling simultaneous consideration of hard data at different scales.

NOMENCLATURE

a	=	range parameter for variogram
a_v	=	range parameter for variogram for data at scale v
C	=	sill parameter for variogram
C^0	=	nugget value for variogram
D^2	=	variance
R	=	large scale region
V	=	volume for coarse scale
v	=	volume for fine scale
σ^2	=	variance for defined scales
$\bullet$	=	point scale
TVD	=	True vertical depth
Γ	=	standard variogram (unit variogram at point-scale)
$\overline{\Gamma}$		average standard variogram value
γ	=	variogram value
$\overline{\gamma}$	=	average variogram for a defined volume
$\overline{\gamma}^*$	=	experimental average variogram value
$\gamma(\mathbf{h})$	=	experimental variogram value for separation distance $\mathbf{h}$
$\mathbf{h}$	=	separation distance vector
$z(\mathbf{u})$	=	variable value at location $\mathbf{u}$
N	=	number of pairs in variogram calculation
Subscripts		
hole	=	hole effect in variogram model
sph	=	spherical structure for variogram model
gau	=	Gaussian structure for variogram model

ACKNOWLEDGMENTS

The authors thank Darwin Ellis and Charles Flaum from Schlumberger-Doll Research for valuable discussions on logging data resolution. We are grateful to the reviewers and editors for their comments and suggestions, especially to David Kennedy whose professional editorial contribution has substantially improved the paper. The authors thank the Geological Survey of Denmark and Greenland (GEUS) for permission to publish.

REFERENCES

Almeida, A. S. and Frykman, P., 1994, Geostatistical modeling of chalk reservoir properties in the Dan Field, Danish North Sea, *in* J. M. Yarus, and R. L. Chambers, eds., *Stochastic Modeling and Geostatistics; Principles, Methods, and Case Studies*: AAPG Computer Applications in Geology, No. 3, The American Association of Petroleum Geologists, Tulsa, p. 273–286.

Andsbjerg, J., 1997, Sedimentology and sequence stratigraphy of Middle Jurassic deposits: Danmarks og Grønlands Geologiske Undersøgelse Rapport 68 (Part 3).

Corbett, P. W. M., Jensen, J. L., and Sorbie, K. S., 1998, A review of up-scaling and cross-scaling issues in core and log data interpretation and prediction, *in* P. K. Harvey and M. A. Lovell, eds., *Core-Log Integration*: Geological Society Special Publications, Geological Society, London, p. 9–16.

Cox, D. L., Lindquist, S. J., Bargas, C. L., Havholm, K. G., and Srivastava, R. M., 1995, Integrated modeling for optimum management of a giant gas condensate reservoir, Jurassic eolian Nugget Sandstone, Anschutz Ranch East Field, Utah Overthrust (U.S.A.), *in* J. M. Yarus, and R. L. Chambers, eds., *Stochastic Modeling and Geostatistics; Principles, Methods, and Case Studies*: AAPG Computer Applications in Geology, No. 3, American Association of Petroleum Geologists, Tulsa, p. 287–321.

Damsleth, E. and Tjølsen, C. B., 1994, Scale consistency from cores to geologic description: *SPE Formation Evaluation*, p. 295–299.

Deutsch, C. V. and Journel, A. G., 1998, GSLIB - Geostatistical Software Library and User's guide: Oxford University Press, New York City, 369 p.

Flaum, C., Galford, J. E., and Hastings, A., 1989, Enhanced vertical resolution processing of dual detector gamma-gamma density logs: *The Log Analyst*, vol. 30, no. 3, p. 139–149.

Flaum, C., Holenka, J. M., and Case, C. R., 1991, Eliminating the rugosity effect from compensated density logs by geometrical response matching: *SPE Formation Evaluation*, v. 6, no. 2, p. 252–258.

Fontaine, J. M., Dubrule, O., Gaquerel, G., Lafond, C., and Barker, J., 1998, Recent developments in geoscience for 3D earth modelling, SPE 50568: Society of Petroleum Engineers, presented at SPE European Petroleum Conference, p. 13–22.

Frykman, P., 2001, Spatial variability in petrophysical properties in Upper Maastrichtian chalk outcrops at Stevns Klint, Denmark: *Marine and Petroleum Geology*, vol. 18, p. 1041–1062.

Frykman, P. and Deutsch, C. V., 1996, Reservoir modelling of the Dan Field accounting for areal trends and scaling of petrophysical properties. Joint Chalk Research, presented at Fifth North Sea Chalk Symposium, 21 p.

Frykman, P. and Deutsch, C. V., 1999, Geostatistical scaling laws applied to core and log data. SPE 56822: Society of Petroleum Engineers, presented at SPE Annual Technical Conference and Exhibition, 12 p.

Gomez-Hernandez, J. J. and Journel, A. G., 1994, Stochastic characterization of grid-block permeabilities: *SPE Formation Evaluation*, vol. 9, no. 2, p. 93–99.

Goovaerts, P., 1997, *Geostatistics for Natural Resources Evaluation*: Oxford University Press, New York, 487 p.

Gringarten, E. and Deutsch, C. V., 2001, Variogram interpretation and modeling: *Mathematical Geology*, vol. 33, no. 4, p. 507–534.

Isaaks, E. H. and Srivastava, R. M., 1989, *An Introduction to Applied Geostatistics*: Oxford University Press, New York, 561 p.

Jennings, J. W. J., 1999, How much core-sample variance should a well-log reproduce: *SPE Reservoir Evaluation & Engineering*, vol. 2, no. 5, p. 442–450.

Journel, A. G. and Huijbregts, C., 1978, *Mining geostatistics*: Academic Press, New York City, 600 p.

Kristensen, L., Dons, T., Maver, K., and Schiøler, P., 1995, A multidisciplinary approach to reservoir subdivision of the Maastrichtian chalk in the Dan Field, Danish North Sea: *American Association of Petroleum Geologists Bulletin*, vol. 79, no. 11, p. 1650–1660.

Kupfersberger, H., Deutsch, C. V., and Journel, A. G., 1998, Deriving constraints on small-scale variograms due to variograms of large-scale data: *Mathematical Geology*, vol. 30, no. 7, p. 837–852.

Massonat, G. J., Poujool, L., and Rebelle, M., 1999, The missing scale: A policy U-turn is necessary in its management, SPE 56820: Society of Petroleum Engineers, presented at 1999 SPE Annual Technical Conference and Exhibition, 15 p.

Oz, B., Deutsch, C. V., and Frykman, P., 2002, A Visual Basic program for histogram and variogram scaling: *Computers & Geosciences*, vol. 28, p. 21–31.

Scholle, P. A., T., A., and Tirsgaard, H., 1998, Formation and diagenesis of bedding cycles in uppermost Cretaceous chalks of the Dan Field, Danish North Sea: *Sedimentology*, vol. 45, p. 223–243.

Stage, M., 2001, Magnetic susceptibility as carrier of a climatic signal in chalk: *Earth and Planetary Science Letters*, vol. 188, p. 17–27.

Sweet, M. L., Blewden, C. J., Carter, A. M., and Mills, C. A., 1996, Modeling heterogeneity in a low-permeability gas reservoir using geostatistical techniques, Hyde Field, Southern North Sea: *American Association of Petroleum Geologists Bulletin*, vol. 80, no. 11, p. 1719–1735.

Tidwell, V. C. and Wilson, J. L., 2000, Heterogeneity, permeability patterns, and permeability upscaling: Physical characterization of a block of Massillon Sandstone exhibiting nested scales of heterogeneity: *SPE Reservoir Evaluation & Engineering*, vol. 3, no. 4, p. 283–291.

Tran, T. T., 1995, The "missing scale" and direct simulation of block effective properties: *Journal of Hydrology*, vol. 183, p. 37–56.

Wen, X. H. and Gomez-Hernandez, J., 1998, Upscaling Hydraulic Conductivities in Cross-Bedded Formations: *Mathematical Geology*, vol. 30, no. 2, p. 181–211.

APPENDIX A
THE VARIOGRAM

The variogram is a critical input to geostatistical studies: (1) it is a tool to investigate and quantify the spatial variability of the phenomenon under study by calculating the

experimental variogram from the data available, and (2) the underlying techniques behind most geostatistical estimation or simulation algorithms require an *analytical variogram model*, which they will honor. The variogram reflects our understanding of the heterogeneity pattern and the continuity of facies and petrophysical properties. Heterogeneity can have a very important impact on predicted flow behavior and consequently on the decisions on reservoir management. The best variogram description is not obtained just by fitting an analytical model to the experimental variogram values derived from data, but must also consider knowledge about geological setting.

The variogram is treated in most geostatistical textbooks with varying detail and nomenclature (Isaaks and Srivastava, 1989; Goovaerts, 1997; Deutsch and Journel, 1998), and this appendix is just a brief summary of some main points related to the description and simulation of geological patterns.

Definition of the semivariogram

In geostatistics the statistic that quantifies the measure of variability is the variogram. The variogram increases as the values of properties measured on a set of samples become more dissimilar. The formula for the "semivariogram" is written conventionally in terms of a "lag" **h**, and a set of observations z, known as attributes, made at a number of locations **x**. The difference in attributes for pairs of spatially separated samples are compared for increasing values of the lag using

$$\gamma(\mathbf{h}) = \frac{1}{2N(\mathbf{h})} \sum_{i=1}^{N(\mathbf{h})} \left(z(x_i + \mathbf{h}) - z(x_i) \right)^2 \qquad \text{(A.1)}$$

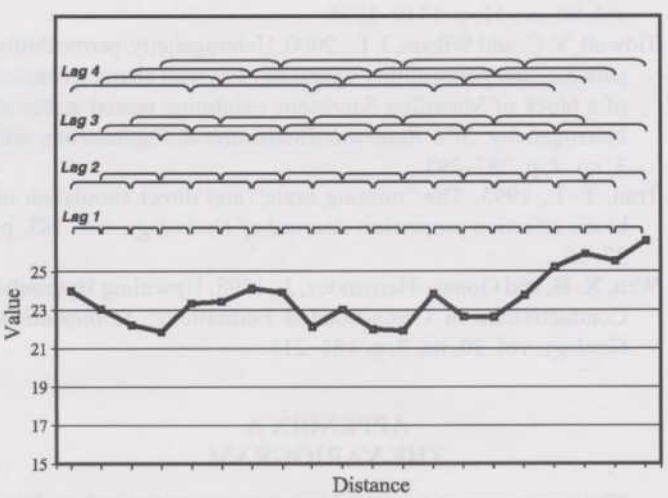

FIG. A.1 Calculation of the variogram values for regularly spaced data. Data pairs are compared for each lag distance.

where the $N(\mathbf{h})$ is a count of the possible pairing at each lag used to compute the function. The variogram is truncated at the value of lag where the diminishing number of possible pairings loses statistical significance. The variogram thus defined can be applied to irregularly spaced observations distributed in two-, or even three-, dimensional space. However, for regularly spaced, colinear observations available from well logs (A.1) can be translated into a simple computational recipe.

For example, for $\mathcal{N}$ regularly spaced observations with an interval denoted by Δ there will be $N = \mathcal{N} - 1$ intervals with lag Δ, $N = \mathcal{N} - 2$ intervals with lag 2Δ, ... , and $N = \mathcal{N}/2$ intervals with lag $\mathcal{N}/2$ if $\mathcal{N}$ is even, or $N = (\mathcal{N} + 1)/2$ intervals with lag $\mathcal{N} - 1/2$ if $\mathcal{N}$ is odd. Denoting the jth value of the lag as h_j, with the corresponding number of samples denoted by N_j, then

$$\gamma(h_j) = \frac{1}{2N_j} \sum_{i=1}^{N_j} \left(z(x_i + h_j) - z(x_i) \right)^2 \qquad \text{(A.2)}$$

where $1 \le j \le \mathcal{N}/2$ or $1 \le j \le (\mathcal{N} + 1)/2$ depending upon whether $\mathcal{N}$ is even or odd, respectively. Finally, $\gamma(h_j)$ is plotted against h_j. With proper attention to the interpretation of the lags, this same formula would apply to irregularly spaced data such as is collected from core plugs.

The strict definition of the variogram is twice the semivariogram or $2\gamma(\mathbf{h})$, but for convenience the semivariogram is usually referred to as the "variogram" except where mathematical rigor requires a precise definition.

Calculating the experimental variogram from data

As mentioned above, one of the first steps in geostatistical studies is to calculate the experimental variogram from the available data. These data are often irregularly sampled data, or they might be found on a regular grid. Since the orientation is very important for analyzing the spatial correlation, the variogram calculation is usually directed in specified directions, most commonly into a vertical and a horizontal variogram. For a simple illustration, data from a 1D example is used in the following.

The principles for calculating the experimental variogram from regularly spaced data are illustrated in Figure A.1. For lag distance = 1 the squared differences for all pairs are summed and divided by $2N$; (N = number of pairs, in this case 19 pairs exist with separation distance 1). This gives the first point for the variogram in Figure A.2. The point for lag = 2 is calculated by comparing points with spacing of 2, and so forth.

This case is easy to illustrate due to the 1D geometry and the regular lags (as it would be for logging data). For irregularly spaced values, the lag distance has a tolerance

interval within which the values are considered. For 3D data a tolerance is needed for both the separation distance and the orientation angle of the distance measurement.

Variogram terminology

The experimental variogram points are not used directly in subsequent geostatistical steps; a parametric variogram model is fitted to the experimental points. A requirement is that we have a variogram measure $\gamma(\mathbf{h})$ for all distance and direction vectors ($\mathbf{h}$) that has the mathematical property of positive definiteness, that is, we must be able to use the variogram in kriging and stochastic simulation. The positive definite model ensures that the kriging equations can be solved and that the kriging variance is positive. For these reasons there are specific positive definite functions such as the spherical, exponential, Gaussian, and hole effect variogram models that are commonly used.

Variogram modeling involves skilled decision-making, but there is a systematic procedure for variogram modeling (Gringarten and Deutsch 2001).

Simple parametric model types are available to model the variogram (Figure A.3). For a given model some basic terms are used to describe the variogram model shape (Figure A.4). The "nugget" value is the variance at a lag distance just larger than 0, and signifies noise or unresolved fine-scale structure. The "sill" is the variance level where the variogram stabilizes. The correlation "range" is the lag distance where the sill is reached. As shown on Figure A.3 the spherical model has a well-defined range, but for the two other model types, exponential and Gaussian, a "practical range" is used where 95% of the sill is reached.

Some variograms show a periodic component, called a "hole effect" (Figure A.5) where the first trough signifies the wavelength of the periodic signal.

The simple variogram shapes introduced here can be combined as "nested structures" to reproduce more complicated experimental variogram shapes. Moreover, the range of continuity can be different in orthogonal directions. The vertical range is usually 1-3 orders of magnitude smaller than the horizontal range.

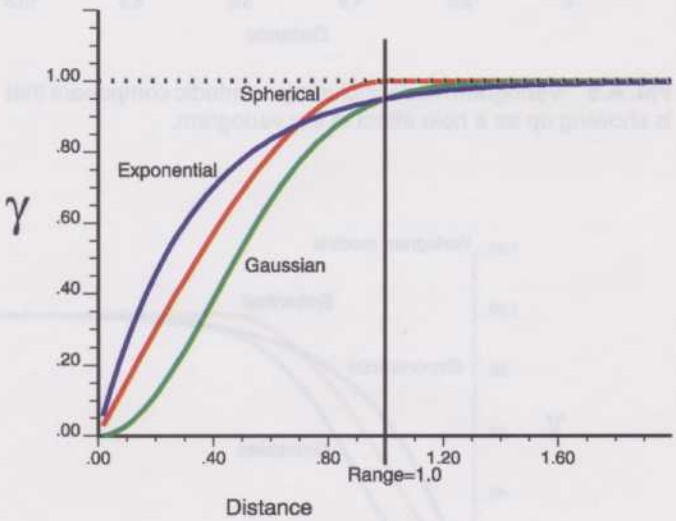

FIG. A.3 The most commonly used analytical variogram models shown with a practical range of 1 m.

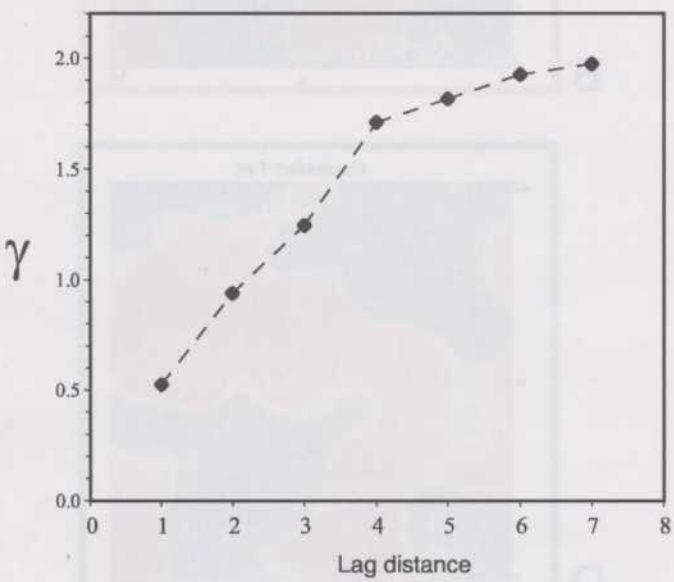

FIG. A.2 The experimental variogram calculated from the data shown in Figure A.1.

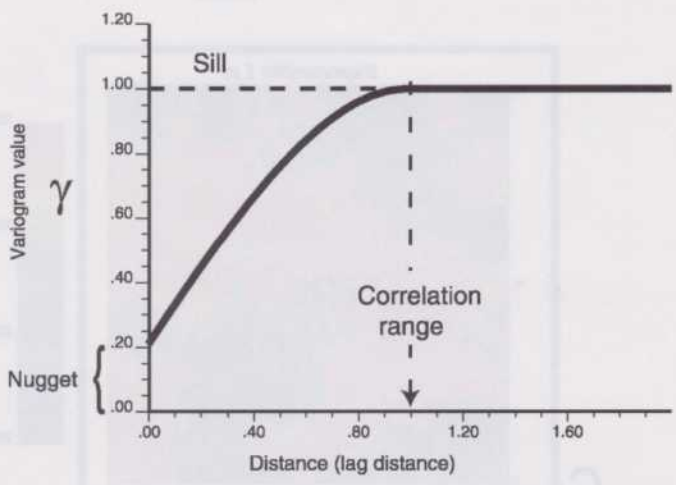

FIG. A.4 Illustration of the terminology used for a variogram model.

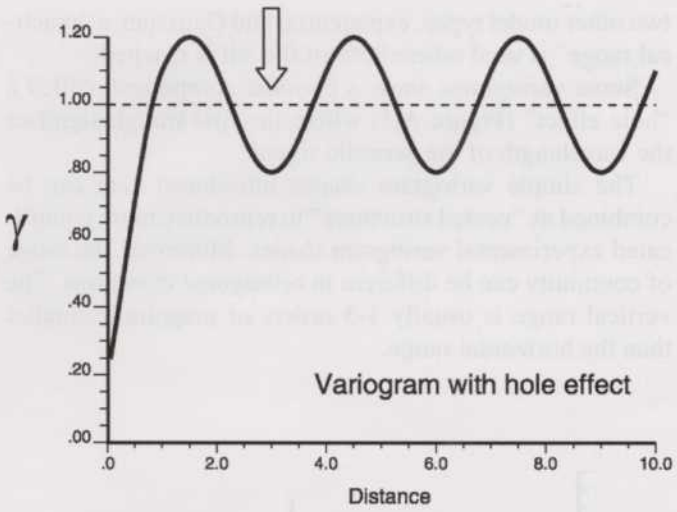

FIG. A.5 Variogram model including a periodic component that is showing up as a hole effect in the variogram.

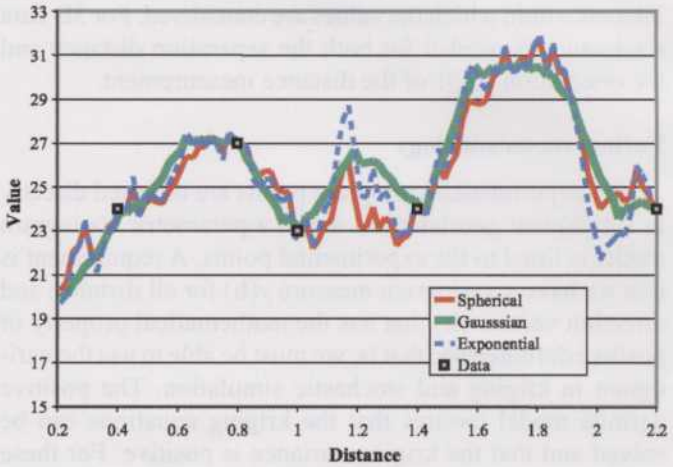

FIG. A.6 Simulation in 1D using the three different variogram models with the same range and sill values.

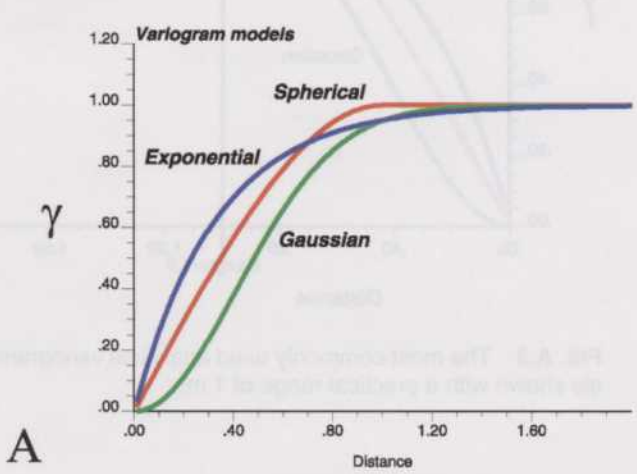

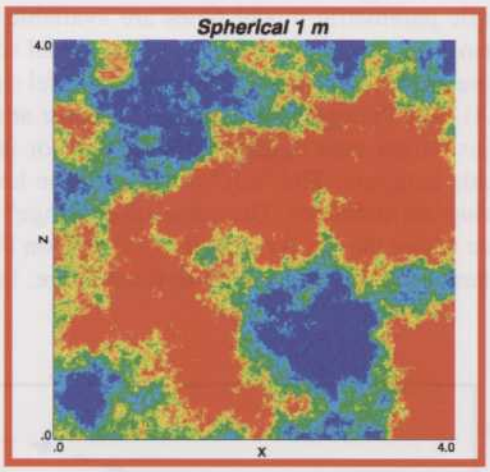

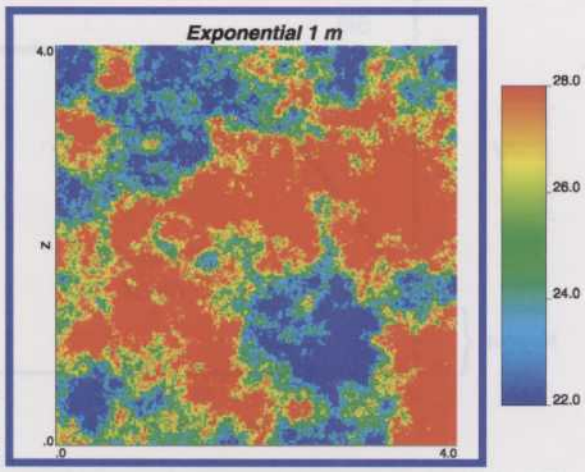

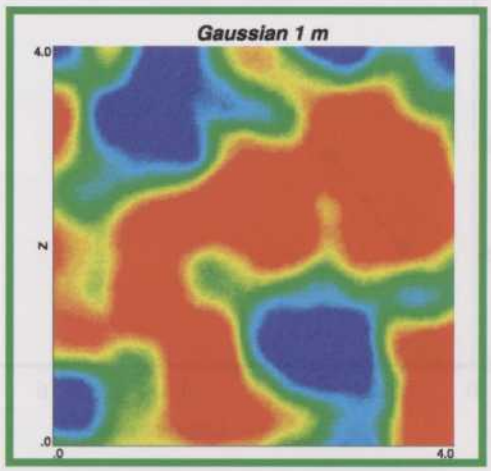

FIG. A.7 Simulation in 2D using the three common variogram models with the same range and sill values.

Stochastic simulation using a variogram model

The variogram model is an important tool together with the target histogram and actual data measurements. The three different variogram models of Figure A.3 will produce different simulated realizations even using the same other input data. This is shown for a 1D example in Figure A.6 and for a 2D example in Figure A.7. The exponential model gives a simulation that looks "noisy," which is due to the steep increase in variance for small distances in the variogram model. The Gaussian variogram model gives a much smoother result, and the spherical model is an intermediate form.

The very different behavior of the three commonly used models are shown especially for 2D modeling in Figure A.7. Therefore, variogram models should not be constructed or chosen by mere fitting to points from the experimental calculation, but should be selected according to the expected pattern in the specific data type that is under evaluation. For the best selection, expert knowledge and qualitative data from analogues form the best support.

ABOUT THE AUTHORS

Peter Frykman is a senior research geologist in the Reservoir Geology Department at the Geological Survey of Denmark and Greenland. He has a special interest in data integration and application of geostatistics in modeling of the North Sea chalk reservoirs, and has worked with characterization at a wide range of scales. He holds a PhD in carbonate sedimentology at the University of Copenhagen. He is a member of SPE and SPWLA.

Peter may be contacted at pfr@geus.dk

Clayton V. Deutsch is a professor in the Department of Civil and Environmental Engineering at the University of Alberta. He teaches and conducts research in geostatistics. He is the director of the Centre for Computational Geostatistics (CCG), an industrial affiliates program. Prior to joining the University of Alberta, Dr. Deutsch was an associate professor (Research) in the Department of Petroleum Engineering at Stanford University and director of the Stanford Center for Reservoir Forecasting (SCRF). He also worked for Exxon Production Research Company and Placer Dome Inc. Dr. Deutsch has published two books and over 40 peer-reviewed technical papers. He holds a PhD in Geostatistics from Stanford University.